Received: 17 May 2023 | Accepted: 5 July 2023

DOI: 10.1002/rmb2.12527

Reproductive Medicine and Biology

WILEY

ORIGINAL ARTICLE

Corroborating evidence for aberrant expression of histone deacetylase 8 in endometriosis

Hanxi Zheng[1] | Xishi Liu[1,2] | Sun-Wei Guo[2,3]

[1]Department of Gynecology, Shanghai Obstetrics and Gynecology Hospital, Fudan University, Shanghai, China

[2]Shanghai Key Laboratory of Female Reproductive Endocrine-Related Diseases, Fudan University, Shanghai, China

[3]Research Institute, Shanghai Obstetrics and Gynecology Hospital, Fudan University, Shanghai, China

Correspondence
Sun-Wei Guo, Research Institute, Shanghai Obstetrics and Gynecology Hospital, Fudan University, Shanghai 200011, China.
Email: hoxa10@outlook.com

Present address
Hanxi Zheng, Gusu School, Center for Human Reproduction and Genetics, Affiliated Suzhou Hospital of Nanjing Medical University, Suzhou Municipal Hospital, Nanjing Medical University, Suzhou, China

Funding information
National Natural Science Foundation of China, Grant/Award Number: 82071623; Shanghai Hospital Development Center, Grant/Award Number: SHDC2020CR2062B

Abstract

Purpose: The aim of this study was to evaluate the dynamic change in staining of Class I HDACs and Hdac6 in lesions harvested serially from different time points in mice with induced endometriosis. In addition, the effect of Hdac8 activation as well as Hdac8 and Hdac6 inhibition on lesional progression and fibrogenesis was evaluated.

Methods: Immunohistochemistry analysis of Class I HDACs and Hdac6 in serially harvested lesion samples in mouse. Hdac8 activation, as well as Hdac6/8 inhibition, was evaluated in mice with induced endometriosis.

Results: We found a progressive increase in lesional staining of Hdac1, Hdac8, and Hdac6 and gradual decrease in Hdac2 staining and consistently reduced staining of Hdac3 during the course of lesional progression. The stromal Hdac8 staining correlated most prominently with all markers of lesional fibrosis. Hdac8 activation significantly accelerated the progression and fibrogenesis of endometriotic lesions. In contrast, specific inhibition of Hdac8 or Hdac6, especially of Hdac8, significantly hindered lesional progression and fibrogenesis.

Conclusions: Hdac8 is progressively and aberrantly overexpressed as endometriotic lesions progress. This, along with the documented HDAC1 upregulation in endometriosis and the overwhelming evidence for the therapeutic potentials of HDACIs, calls for further and in-depth investigation of epigenetic aberrations of endometriosis in general and of HDACs in particular.

KEYWORDS
endometriosis, fibrogenesis, histone deacetylase 8, mouse, progression

1 | INTRODUCTION

Endometriosis is a common gynecological disease affecting mostly women of reproductive age and a leading contributor to pelvic pain and subfertility.[1] It is an estrogen-dependent disease,[2] and the treatment of choice is based on altering the hormonal milieu of the menstrual cycle with the goal to induce a state of pseudo-pregnancy, pseudo-menopause, or chronic anovulation, creating an acyclic hypoestrogenic environment.[3] Endometriosis has also been recognized as an inflammatory disease.[4] Unfortunately, all clinical trials on non-hormonal, anti-inflammatory drugs for endometriosis have failed or are presumed to be failed so far.[5]

Endometriosis also has been proposed to be an epigenetic disease,[6] featuring epigenetic aberrations.[7–9] Indeed, various

This is an open access article under the terms of the Creative Commons Attribution-NonCommercial License, which permits use, distribution and reproduction in any medium, provided the original work is properly cited and is not used for commercial purposes.
© 2023 The Authors. *Reproductive Medicine and Biology* published by John Wiley & Sons Australia, Ltd on behalf of Japan Society for Reproductive Medicine.

epigenetic aberrations in endometriosis have been reported,[10–15] including genes/proteins involved in epigenetic modifications, such as histone deacetylases (HDACs),[16,17] DNA methyltransferases (DNMTs),[18,19] and various histone modifiers.[20–25] In particular, HDAC inhibitors (HDACIs) have been demonstrated in preclinical studies to be a promising therapeutic.[13,26–39] This line of research culminated in the successful proof-of-concept clinical application of valproic acid (VPA), a mood stabilizer and an HDACI, in treating adenomyosis.[40,41]

As of today, 18 human HDACs have been identified, which can be grouped into four classes: Class I consists of HDAC1-3 and 8, Class II consists of HDAC4-7, 9 and 10, Class III consists of SIRT1-7, and Class IV consists of HDAC11.[42] Histone acetylation is an integral part of epigenetic modification and is synergistically regulated by histone acetyltransferase (HAT) and HDAC, both of which are involved in various aspects of health and disease.[43]

In endometriosis, however, only Classes I and III HDACs have been investigated so far, albeit incompletely. Still, results are anything but congruent: one study reported that both HDAC1 and HDAC2 are overexpressed in endometriosis,[44] another study only found HDAC1, but not HDAC2, overexpression.[16] A recent study reported lesional overexpression of HDAC2, and its silence prevents endometriosis.[45] In eutopic endometrium, downregulation of HDAC3 in infertile women with endometriosis has been reported.[46] However, no other Classes I, II, and IV HDACs have been investigated.

In addition to the many desirable features of HDACIs such as anti-proliferative and anti-inflammatory propensity and its capability to reactivate silenced PR-B,[13,26–39] HDACIs have been shown to suppress uterine contraction,[32,47,48] attenuate inflammation,[49] and contain fibrosis.[50–54] Uterine hyperactivity is a well-recognized contributor to dysmenorrhea,[55] and fibrosis has emerged fairly recently as one important hallmark of endometriosis.[56,57] These desirable properties make HDACIs a very promising therapeutic.

VPA only targets Class I (HDAC1-3 and 8) and Class IIa (HDAC4-5, 7, and 9) HDACs.[58,59] It is certainly not the best HDACI for treating endometriosis since it is a Category D drug, even though it has a rapid clearance.

Growing data accumulated in the last 5–6 years indicate that endometriotic lesions are not monolithic. As lesions undergo repeated tissue injury and repair (ReTIAR), they progress through epithelial–mesenchymal transition (EMT), fibroblast-to-myofibroblast trans differentiation (FMT), and smooth muscle metaplasia (SMM), and become progressively more fibrotic.[57,60,61] As such, lesions are highly dynamic, and their cellular identity is by no means immutable, but, rather, changes following cues from the lesional microenvironment. Indeed, different subtypes of endometriosis, such as ovarian endometrioma (OE) and deep endometriosis (DE), often exhibit different molecular signatures.[23,62] Failure to recognize this dynamic nature of endometriotic lesions invariably led to potholes and blind alleys in drug research and development.[5,63] Indeed, prostaglandin E2 (PGE2) signaling, one that is viewed to play a pivotal role in endometriosis as it sits on the nexus linking inflammation and hyperestrogenism,[64] becomes diminished as lesions progress.[65,66]

Therefore, it is highly likely that the conflicting results seen in the endometriosis literature may be an artifact resulting from the failure to account for the lesional developmental stage and the difference between endometriotic epithelial and stromal components. In order to assess the potential of HDACs as a therapeutic target, it is necessary to further investigate the roles of HDACs in endometriosis in the context of lesional progression.

Using in vitro screening that mimics EMT and FMT processes, we have identified among all HDACs except sirtuins that Class I HDACs as well as HDAC6 appeared to be involved in endometriosis (Zheng et al., submitted for publication). Through immunohistochemistry analysis of OE and DE lesion samples as well as gene and protein expression analyses using endometriotic epithelial cells and primary endometriotic stromal cells derived from OE lesions, we found nuanced overexpression of HDAC1, HADC8, and HDAC6 but reduced expression of HDAC2 and HDAC3, depending on the lesional development stage (Zheng et al., submitted for publication). In addition, we found that inhibition of HDAC8 has a therapeutic potential (Zheng et al., submitted for publication).

To further understand the roles of Class I HDACs and HDAC6 in lesional progression, we carried out a serial mouse experiment, evaluating the lesional immunostaining levels of Class I HDACs and Hdac6 in comparison with that of control endometrium. In addition, we evaluated the effect of Hdac8 activation in a mouse model of endometriosis. Finally, we evaluated the effect of inhibition of either Hdac8 or Hdac6 on lesional progression and fibrogenesis. Our results clearly identify Hdac8 as a promising therapeutic target, reaffirming as well as highlighting the therapeutic potential of HDACIs.

2 | METHODS AND MATERIALS

2.1 | Animals

A total of 124 6-week-old virgin female Balb/C mice were purchased from the Shanghai Jiesijie Experimental Animal Company. All mice were maintained under a controlled environment with 22–25°C, a 12-/12-h light/dark cycle, and access to feed and water ad libitum. All experiments were performed under the US National Research Council's Guide for the Care and Use of Laboratory Animals[67] and were approved by the Institutional Experimental Animals Review.

2.2 | Induction of endometriosis

We used a well-established mouse model of endometriosis by intraperitoneal (i.p.) injection of uterine fragments as reported previously.[68,69] Briefly, after 1 week of acclimatization, the donor mice received an intramuscular (i.m.) injection of estradiol benzoate (3 μg/mouse; Animal Medicine Factory, Hangzhou, China) twice a week to stimulate the endometrium growth. One week later, all donor mice were sacrificed by cervical dislocation, and their uteri were harvested. The harvested uterine tissues were seeded in a Petri dish

(Corning, Corning, NY, USA) containing warm sterile saline, split longitudinally with a pair of scissors, and minced until the fragments were no larger than 1 mm^3. The fragments were then injected (i.p.) into the pelvic cavity of the recipient mice. To minimize potential biases, we mixed the uterine tissue fragments from several donor mice and then divided them into several parts (depending on the number of groups), with each i.p. injected into one mouse each from one of experimental groups.

2.3 | Hotplate test

To evaluate the extent of pain resulting from endometriosis, all mice were administrated with the hotplate test using a commercial Hotplate Analgesia Meter (Model BME-480, Institute of Biomedical Engineering, Chinese Academy of Medical Sciences, Tianjin, China) as reported previously.[31] Briefly, mice were allowed to acclimatize for 10 min before the test. The withdrawal latencies to thermal stimulation were determined according to the following criteria: shaking or licking its hind paws or jumping on the hotplate from the moment we initially placed the mouse into the cylinder. The latency was measured twice and then averaged by two test results during a one-hour interval.

2.4 | Protocol for Experiment 1: Serial experiment

A total of 60 mice were used for this experiment. Among these mice, 18 mice were randomly selected as donors and the remaining 42, recipients. Among the 42 recipient mice, six of them were selected at random to serve as controls, receiving only a mock injection of warm sterile saline. Every week until the 6th week after the induction of endometriosis, six mice were sacrificed. For all mice, their bodyweight and hotplate latency were measured before induction (Day 0) and each time before sacrifice (Weeks 1, 2, 3, 4, 5, and 6 post-induction) by cervical dislocation. The control mice were sacrificed at the end of the 3rd week in order to be maximally representative. After sacrifice, the abdominal cavities were immediately cut open, and all visible lesions (or uteri for control mice) were harvested. The total weight of lesions from each mouse was weighed and fixed immediately in fixative and embedded in paraffin for histological and immunohistochemical analyses.

2.5 | Protocol for Experiment 2: Effect of selective activation of Hdac8

A total of 24 mice were used for this experiment, eight of them were randomly selected as donors of uterine tissues, and the remaining 16 were recipients.

For this experiment, we used TM-2-51 (S505528; Sigma-Aldrich, St. Louis, MO, USA), an N-acetylthiourea derivative identified as an HDAC8 activator, exhibiting the highest potency and isoform selectivity.[70] Since there is no literature on its use or other HDAC activators' use in animal experiments, we decided to refer to the dosage, route of administration, and solvent of PCI-34051, a selective HDAC8 inhibitor, which was well tolerated in our animal experiments. TM-2-51 was dissolved in normal saline containing 5% DMSO (Sigma-Aldrich), 30% PEG300 (Sangon Biotech, Shanghai, China), and 0.5% Tween80 (Saiguo Biotech, Guangzhou, China). Its effectiveness was confirmed by a pilot experiment.

The recipient mice were randomly divided into two equal-sized groups, the control group, and the TM-2-51 (20 mg/kg/day) group. Two weeks after the induction of endometriosis, mice were i.p. injected with either TM-2-51 solution every 2 days or an equal volume of solvent in an identical manner. All mice were sacrificed 4 weeks after the induction of endometriosis. The abdominal cavities were immediately cut open, and all visible lesions were carefully excised. The total weight of lesions from each mouse was weighed and fixed immediately in fixative and embedded in paraffin for histological and immunohistochemical analyses. The bodyweight and hotplate latency were measured before and 2 and 4 weeks after the induction.

2.6 | Protocol for Experiment 3: Effect of Hdac6/8 selective inhibition

Among the 40 female adult Balb/C mice, 15 were randomly selected as donors of uterine tissues, and the remaining 25 served as recipients that received endometrial fragments i.p. injection. Herein, Tubastatin A (S8049, Selleck, Houston, TX, USA) and PCI-34051 (S2012, Selleck) were used as the inhibitor of HDAC6 and HDAC8, respectively.

PCI-34051 is the most widely used selective inhibitor of HDAC8.[71] Tubastatin A is a widely used HDAC6 inhibitor that has therapeutic potential in animal models such as neurodegenerative diseases, autoimmune diseases, and cardiovascular diseases.[72] Recent results also showed that it is also a potent HDAC10 inhibitor.[73]

Both inhibitors were dissolved in a solvent composed of 5% DMSO (D2650, Sigma-Aldrich, St. Louis, MO, USA), 30% PEG300 (Sangon Biotech, Shanghai, China), 0.5% Tween80 (Saiguo Biotech, Guangzhou, China), and 64.5% sterile normal saline. The recipient mice were randomly divided into five equal-sized groups: control (CT), low-dose Tubastatin A (LT, 20 mg/kg/day), high-dose Tubastatin A (HT, 40 mg/kg/day), low-dose PCI-34051 (LP, 10 mg/kg/day), and high-dose PCI-34051 (HP, 20 mg/kg/day). One day before the induction of endometriosis, mice in experimental groups were i.p. injected with respective inhibitor-containing solutions, while mice in the CT group received an equal volume of vehicle.

The dosages and administration routes of the inhibitors were determined based on previous reports.[74–80] Designating the day when the endometriosis induction procedure was Day 0, mice in each group received vehicle or inhibitors via i.p. administration once a

day for 2 weeks, starting from Day −1 (1 day before induction), were sacrificed by cervical dislocation on Day 14 after the induction. The bodyweight and hotplate latency were measured on Days −1, 0, 7, and 14 after the induction.

At the end of the experiment (Day 14), the abdominal cavities were immediately cut open, and all visible lesions were carefully excised. The total weight of excised lesions from each mouse was weighed and fixed immediately in fixative and embedded in paraffin for histological and immunohistochemical analyses.

2.7 | Immunohistochemistry and Masson trichrome staining

Serial 4-μm sections were obtained from each tissue sample, with the first resultant slide being H&E stained to confirm pathologic confirmation, and the subsequent slides for IHC analysis for all members of Class I HDACs (Hdac1-3, and Hdac8), and one member of Class IIa HDACs, Hdac6, E-cadherin (a marker for epithelial cells), vimentin (a marker for mesenchymal cells), α-smooth muscle actin (α-Sma, a marker for myofibroblasts), desmin, smooth muscle myosin heavy chain (Sm-mhc) (two markers of highly differentiated smooth muscle cells or SMCs), and Pcna (a marker for proliferation). The immunohistochemistry procedure and Masson trichrome staining are described in more detail in Appendix S1. The vendor's names and catalog numbers of these antibodies and the dilution ratios are listed in Table S1. For positive control, different tissue slides were used for different antibodies according to the vendor's informative sheet. For negative controls, tissue samples were incubated with rabbit or mouse serum instead of primary antibodies. The representative photomicrographs for positive and negative control are provided in Figure S1.

2.8 | Western blot analysis

Total protein of lesion tissues was extracted by grinding in RIPA lysis buffer (Yeasen, Shanghai, China) with a grinding instrument (Servicebio biotech, Wuhan, China), and the cell-RIPA mixture was centrifuged at ~13 400 *g* for 10 min at 4°C to rid of cell debris. Protein concentration was determined using bicinchoninic acid (BCA) protein quantitative analysis kit (Beyotime Biotech, Shanghai, China). Protein samples were loaded on a 10% SDS-PAGE and transferred to 0.22 μm polyvinyl difluoride (PVDF) membranes (EMD Millipore, Merck, Darmstadt, Germany). The membranes were then incubated with the primary antibodies at 4°C overnight. The information on primary antibodies is listed in Table S2. After the membranes were incubated with secondary antibodies on a shaker for 1.5 h at room temperature, the signals were detected with enhanced chemiluminescence (ECL) kit (New Cell & Molecular Biotech, Suzhou, China) and digitized on Image Quant LAS 4000 mini (GE, Boston, MA, USA). Image quantification was performed using Image J software (Version 1.53a, downloaded from https://imagej.net/Downloads).

2.9 | Statistical analysis

The comparison of distributions of continuous variables between or among two or more groups was made using Wilcoxon's and Kruskal's test, respectively, and the paired Wilcoxon's test was used when the before-after (induction of endometriosis) comparison was made for the same group of subjects. For Experiment 1, multivariate linear regression analyses were used to determine which factors were associated with lesion weight, hotplate latency or immunostaining levels. For Experiment 3, since we did not intend to determine exactly which dosage is effective but merely intended to know whether it has the suppressive effect and whether there is a dose–response relationship, we also employed multiple linear regression using the dosage of either Tubastatin A treatment (20 vs. 40 mg/kg/day) or PCI-34051 treatment (10 vs. 20 mg/kg/day) as two independent variables. This analysis could also fully use the data and to minimize the risk of type I error due to multiple testing. Similar analysis was also used for Experiment 1 data when protein expression levels of tissues collected at different time points were evaluated. When a statistically significant linear trend was detected, a red arrow was used to illustrate this trend. *p*-values of <0.05 were considered statistically significant. All computations were made with R 4.2.2.[81]

3 | RESULTS

3.1 | Overexpression of Hdac8 during lesional progression

We first conducted a serial mouse experiment and evaluated the lesional staining of Class I HDACs and Hdac6. No mouse died during the entire course of the experiment. Endometriosis was successfully induced and histologically confirmed by H&E staining. Among mice with induced endometriosis, the bodyweight increased progressively with time ($p=3.7\times10^{-8}$; $R^2=0.59$; Figure 1A), although their bodyweight prior to the induction was significantly lower than that of control mice without endometriosis measured at Week 3 ($p=0.037$). The lesion weight also increased progressively with the duration of induction, and starting from Week 3 after induction, the lesion weight was significantly heavier than that of Week 1 ($p=0.026$, $p=0.087$, $p=0.015$, and $p=0.0022$; Figure 1B). A multiple linear regression analysis incorporating the week at which tissue samples were harvested, bodyweight at the time of harvest, and their interaction indicated that the lesion weight increased progressively as the time elapsed from the induction of endometriosis ($p=1.2\times10^{-5}$, $R^2=0.44$; Figure 1B). In contrast, the hotplate latency decreased progressively ($p=2.0\times10^{-12}$, $R^2=0.51$; Figure 1C), consistent with results previously reported.[82] In addition, while the baseline latency (Week 0) from mice with endometriosis was similar to that of control mice evaluated at Week 3 ($p=0.77$), the latency in endometriosis mice was either significantly or marginally shorter starting from Week 1 after induction (all *p*-values = 0.031 except at Weeks 1 and 4, in which both *p*-values = 0.063; Figure 1C).

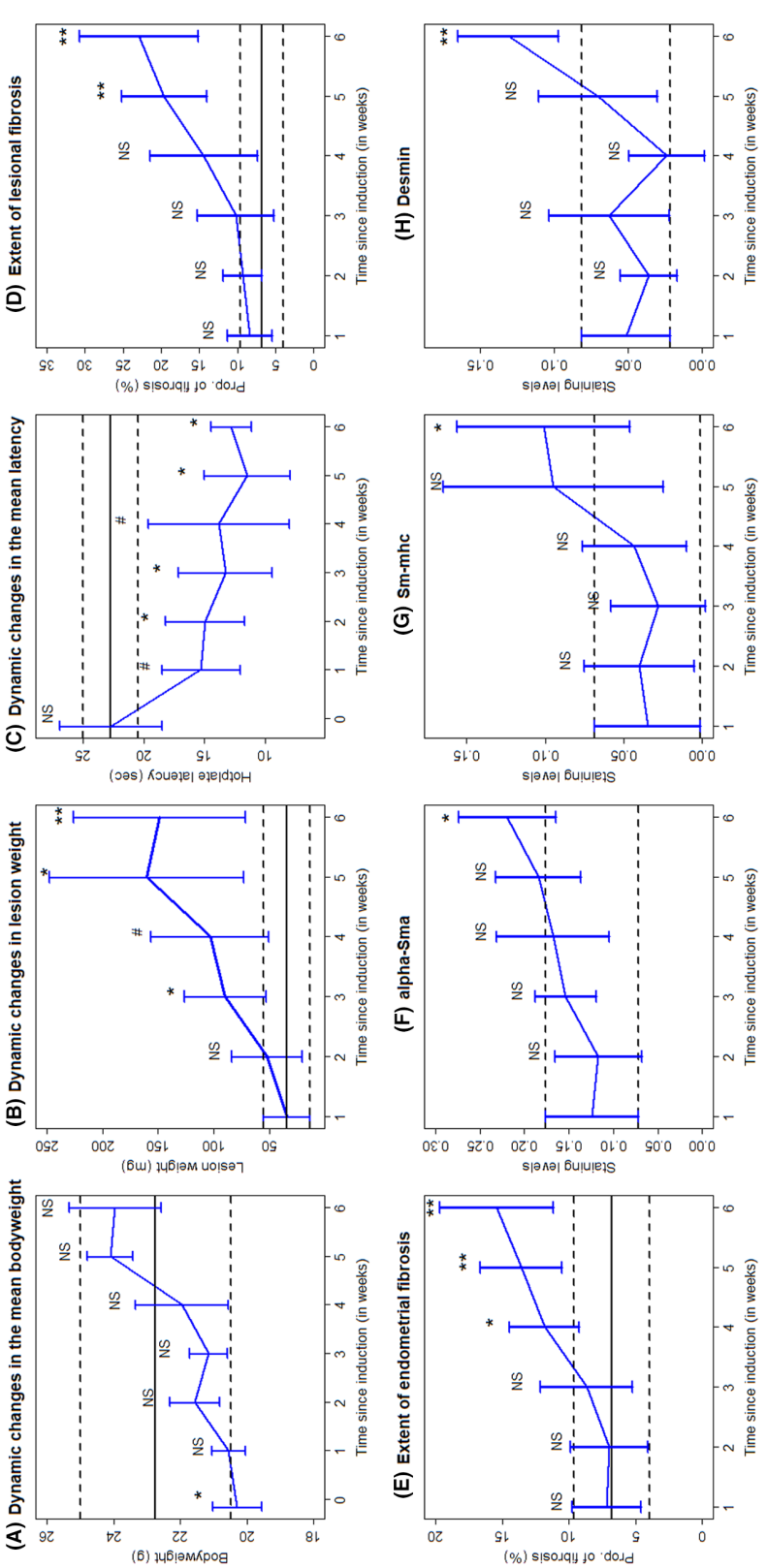

FIGURE 1 Dynamic changes in the mean bodyweight (A), lesion weight (B), the hotplate latency (C) of mice, and the extent of lesional fibrosis (D), extent of endometrial fibrosis (E), α-Sma (F), desmin (G), and Sm-mhc (H) in serially harvested endometriotic lesions of mice with induced endometriosis and mouse uteri (of control mice) during the progression of endometriosis. The data are represented by the means ± SDs. In panels of (A) and (C), the solid line represents the mean value of the control mice, while the dashed lines represent the mean ± SDs. For panels (D) and (E), the solid and dashed lines represent the mean and the mean ± SDs of the staining levels of endometrium from all control mice. In the remaining panels, the lines representing the mean and mean ± SDs represent the data collected at Week 1 after the induction of endometriosis. Symbols of statistical significance levels: #: $0.05 < p < 0.1$; *: $p < 0.05$; **: $p < 0.01$; NS: $p > 0.05$. $N = 6$ in each group. All comparison was made using Wilcoxon's test.

We also conducted Masson trichrome staining to evaluate the extent of fibrosis in ectopic and eutopic endometrium as well as immunohistochemistry analysis of α-Sma, Sm-mhc, and desmin in endometriotic tissue samples, using the endometrium from control mice harvested 3 weeks after induction as reference (Figure 2). Sm-mhc and desmin are two markers of highly differentiated SMCs. α-Sma staining was seen primarily in the endometriotic stromal component, and Sm-mhc and desmin staining was seen mostly in the cytoplasm of the stromal component in ectopic endometrium.

We found that the extent of fibrosis increased progressively as the time elapsed from the induction ($p = 0.0021$, $R^2 = 0.25$; Figure 1D), reaching to an average of nearly 25% by the end of the 6th week. While the extent of lesional fibrosis did not differ significantly from the extent of endometrial fibrosis in control mice (evaluated at Week 3) during the first 4 weeks after induction (all four p-values $\geqq 0.093$; Figure 1D), starting from Week 5, the extent of lesional fibrosis became significantly higher (both p-values ≤ 0.002). In addition, the extent of fibrosis in eutopic endometrium also increased progressively

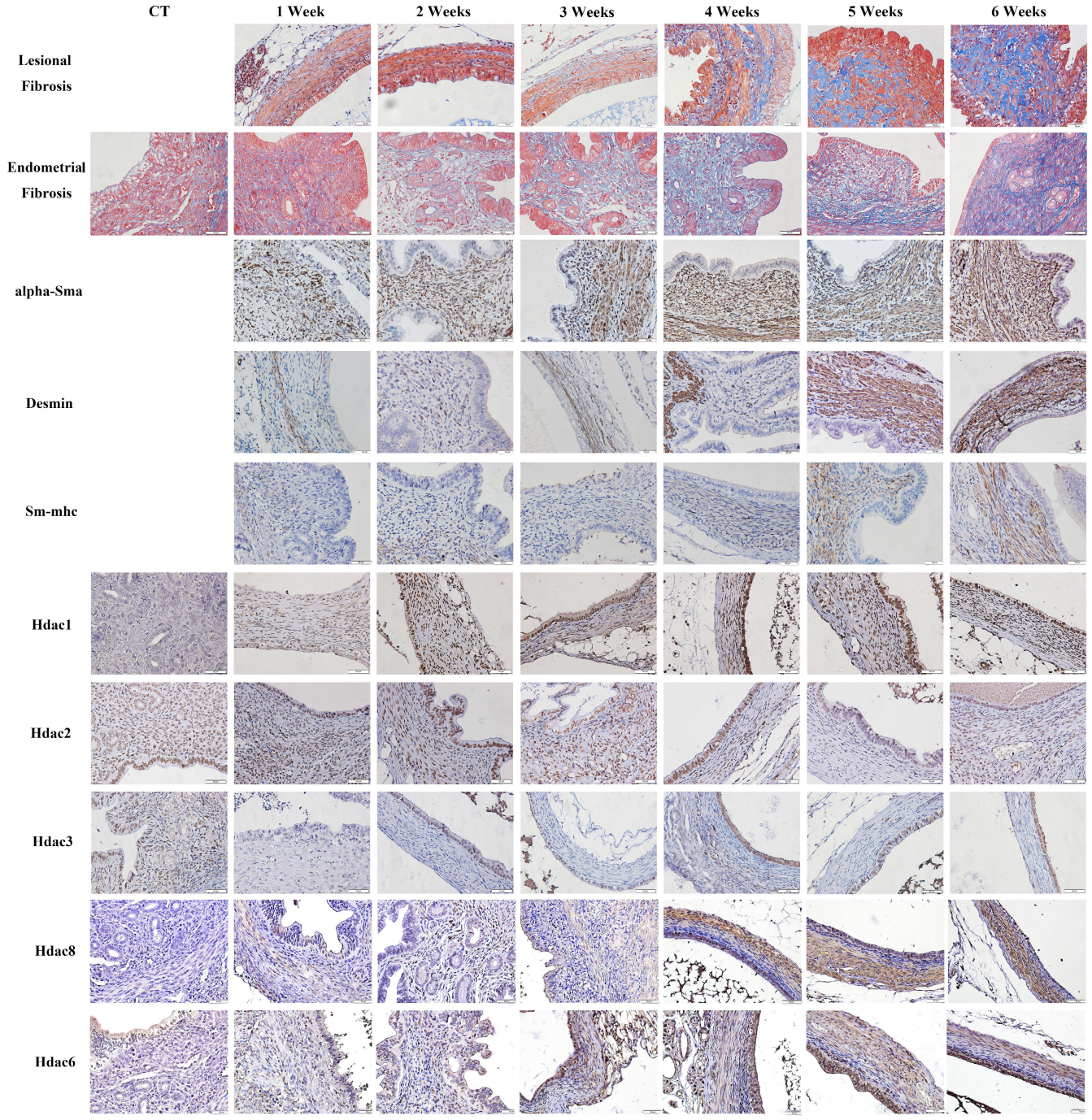

FIGURE 2 Representative immunostaining and Masson trichrome photomicrographs in Experiment 1. Different rows show different markers as indicated. Different columns represent different tissue samples, that is, endometrium from control mice (CT) and endometriotic lesions of endometriosis mice. In all figures, magnification: ×400. Scale bar = 50 μm.

although at much lower levels ($p=8.3\times10^{-10}$, $R^2=0.61$; Figure 1E). In particular, while the extent of endometrial fibrosis did not differ significantly from that of control mice (evaluated at Week 3) during the first 3 weeks after induction (all three p-values ≧0.24; Figure 1E), starting from Week 4, the extent of endometrial fibrosis was significantly higher (all three p-values ≤0.015). For mice with induced endometriosis, the extent of lesional fibrosis and of endometrial fibrosis were positively correlated ($r=0.63$, $p=4.3\times10^{-10}$).

Consistent with the gradual but progressive EMT and FMT as shown in in vitro studies,[60,61] we found that the immunostaining levels of α-Sma increased slowly but progressively ($p=0.0002$, $R^2=0.34$; Figure 1F). Consistent with previously reported,[82] the extent of desmin- or Sm-mhc-positive SMCs or the extent of SMM also increased progressively ($p=0.003$, $R^2=0.25$, and $p=0.007$, $R^2=0.20$; Figure 1G,H), starting from 5 to 6 weeks after the induction.

As expected, the extent of lesional fibrosis correlated positively with that staining levels of α-Sma, Sm-mhc, and desmin ($r=0.69$, $p=3.9\times10^{-6}$, $r=0.53$, $p=0.0014$, and $r=0.61$, $p=8.2\times10^{-5}$, respectively). The extent of lesional fibrosis also correlated positively with the lesion weight ($r=0.51$, $p=0.0015$) but negatively with the hotplate latency ($r=-0.37$, $p=0.027$).

We also performed the IHC analysis of all 4 members of Class I HDACs and Hdac6 in endometriotic lesions as compared to the endometrial samples from the control mice. We observed the dynamic changes of Hdac1, Hdac2, Hdac3, Hdac8, and Hdac6 staining in serially harvested endometriotic lesions (Figure 2). We found that the staining of Hdac1, Hdac2, Hdac3, Hdac8, and Hdac6 was seen in both epithelial and stromal cells. Hdac1 and Hdac2 staining was localized in the cellular nucleus, Hdac3 and Hdac8 were in the nuclei and cytoplasm, while Hdac6 was in the cytoplasm (Figure 2). The staining levels were summarized separately by the glandular epithelial and stromal components.

In general, the staining intensity of all HDACs evaluated was higher in the epithelial component than that in the stromal component (Figure 3), although the staining levels were all positively correlated between the two components (all r's ≥ 0.38, all p-values ≤0.014). Hdac1 staining was quickly and significantly elevated in the glandular epithelial component as lesions progressed ($p=1.4\times10^{-6}$, $R^2=0.66$), starting from the 2nd week after the induction as compared with the control endometrium (all p-values ≤0.04; Figure 3A), whereas that in the stromal component became significantly elevated starting from Week 4 after induction (all p-values ≥0.24 before Week 4, then all p-values <0.041; Figure 3B). The trend for progressive increase in the stroma was found to be statistically significant by linear regression ($p=0.0043$, $R^2=0.22$).

In contrast, we did not observe any significant changes in Hdac2 staining in lesions in either epithelial or stromal component as lesions progressed (all p-values ≥0.10; Figure 3C,D). Despite the lack of difference, there was a linearly decreasing trend in lesional staining in both the epithelial and stromal components (both p-values ≤0.005, both R^2 ≧ 0.21; Figure 3C,D).

In both epithelial and stromal components, there was no trend in the Hdac3 staining levels as lesions progressed (two p-values >0.77, $R^2<0.005$). In the epithelial component, Hdac3 staining levels were significantly lower at Weeks 1, 3, and 6 than that of control endometrium (all p-values ≤0.015; Figure 3E). Similarly, its staining levels were all significantly lower than that of the control endometrium starting from just 1 week after induction (all p-values ≤0.026; Figure 3F).

The lesional staining of Hdac8 increased gradually and progressively in both epithelial and stromal components during lesion progression ($p=0.011$, $R^2=0.27$, and $p=3.6\times10^{-7}$, $R^2=0.54$, respectively; Figure 3G,H), especially during the later stage. More specifically, Hdac8 staining in the stroma of endometriotic lesions was significantly elevated as lesions progressed, starting from the 4th week after the induction (all three p-values = 0.0022; Figure 3H). In contrast, the elevation started at the 5th week in the epithelial component ($p=0.041$, and $p=0.065$, respectively; Figure 3G).

Similarly, the Hdac6 staining levels in both epithelial and stromal components of endometriotic lesions were significantly elevated as lesions progressed ($p=8.1\times10^{-8}$, $R^2=0.45$, and $p=0.038$, $R^2=0.12$, respectively; Figure 3I,J). In the epithelial component in particular, the Hdac6 staining levels were significantly higher than that of control endometrium starting from the 4th week after induction (all three p-values ≤0.026; Figure 3I) while in the stromal component the staining levels became significantly higher than that of control endometrium at the 6th week ($p=0.009$; Figure 3J).

We found that the extent of lesional fibrosis correlated positively with the lesional staining of Hdac1 in the epithelial component ($r=0.72$, $p=9.2\times10^{-7}$; Figure S2A) and of Hdac8 and Hdac6 in both the epithelial and stromal components (all r's ≥ 0.50, all p-values ≤0.002; Figure S2B–E). In addition, lesional staining of Hdac8 in both epithelial and stromal components correlated positively with that of the FMT marker (α-Sma) and SMM makers (Sm-mhc and desmin) (all r's ≥ 0.49, all p-values ≤0.002; Figure S2F–K). Lesional staining of Hdac8 in epithelium correlated negatively with the hotplate latency ($r=-0.34$, $p=0.040$; Figure S2L).

We also extracted the total tissue protein of serially harvested lesion samples and evaluated the protein expression levels of Hdac1-3, Hdac8, and Hdac6 during the progression of endometriosis via western blot. To ensure enough protein content, we grouped the lesion samples by the length of induction as early (1–2 weeks), middle (3–4 weeks), and late stages (5–6 weeks) (Figure 4A). We found that for Hdac1 and Hdac8, there was an "age"-dependent increase in protein expression levels (both p-values <0.0004, both R^2's ≧ 0.45; Figure 4B) and an "age"-dependent decrease in Hdac2 protein levels ($p=0.049$, $R^2=0.17$; Figure 4B). For Hdac6, the "age"-dependent increase in protein levels was marginally significant ($p=0.066$, $R^2=0.16$; Figure 4B). However, there was no significant difference in the protein levels of Hdac3 ($p>0.3$; Figure 4B), consistent with IHC results since the lesional staining of Hdac3 in the stromal, but not the epithelial, component is consistently and significantly lower than that of control endometrium (Figure 3F).

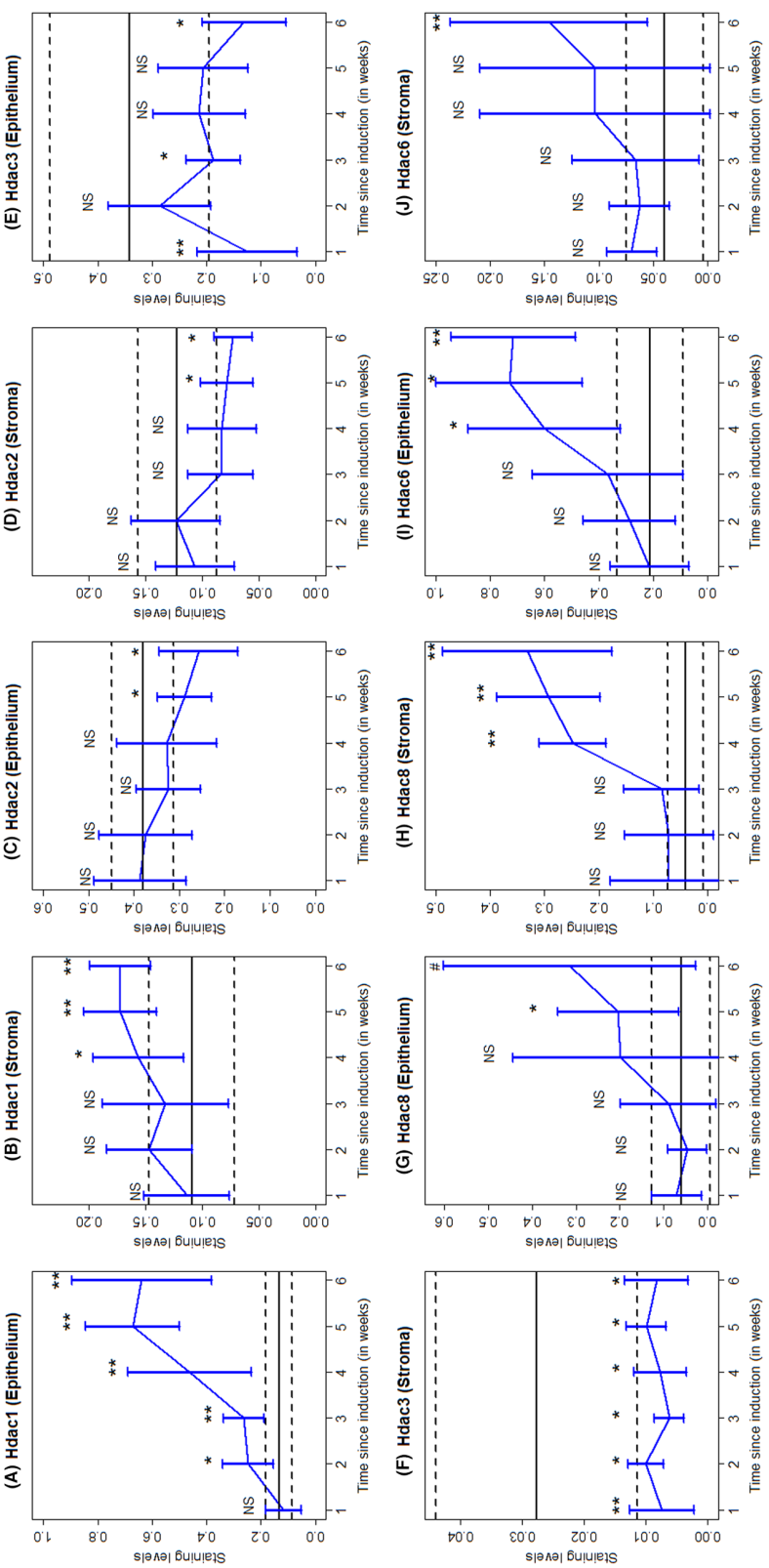

FIGURE 3 Data summary of dynamic changes staining levels of all members of Class I HDACs and Hdac6, scored separated by the epithelial or stromal component in serially harvested lesion samples from mice with induced endometriosis during the progression of endometriosis in Experiment 1. The data are represented by the means ± SDs. In all panels, the solid and dashed lines represent the mean and the mean ± SDs of the staining levels of endometrium from all control mice. Symbols of statistical significance levels: #: $0.05 < p < 0.1$; *: $p < 0.05$; **: $p < 0.01$; NS: $p > 0.05$. $N = 6$ in each group. All comparison was made in reference to the staining levels of the control endometrium, using the Wilcoxon's test.

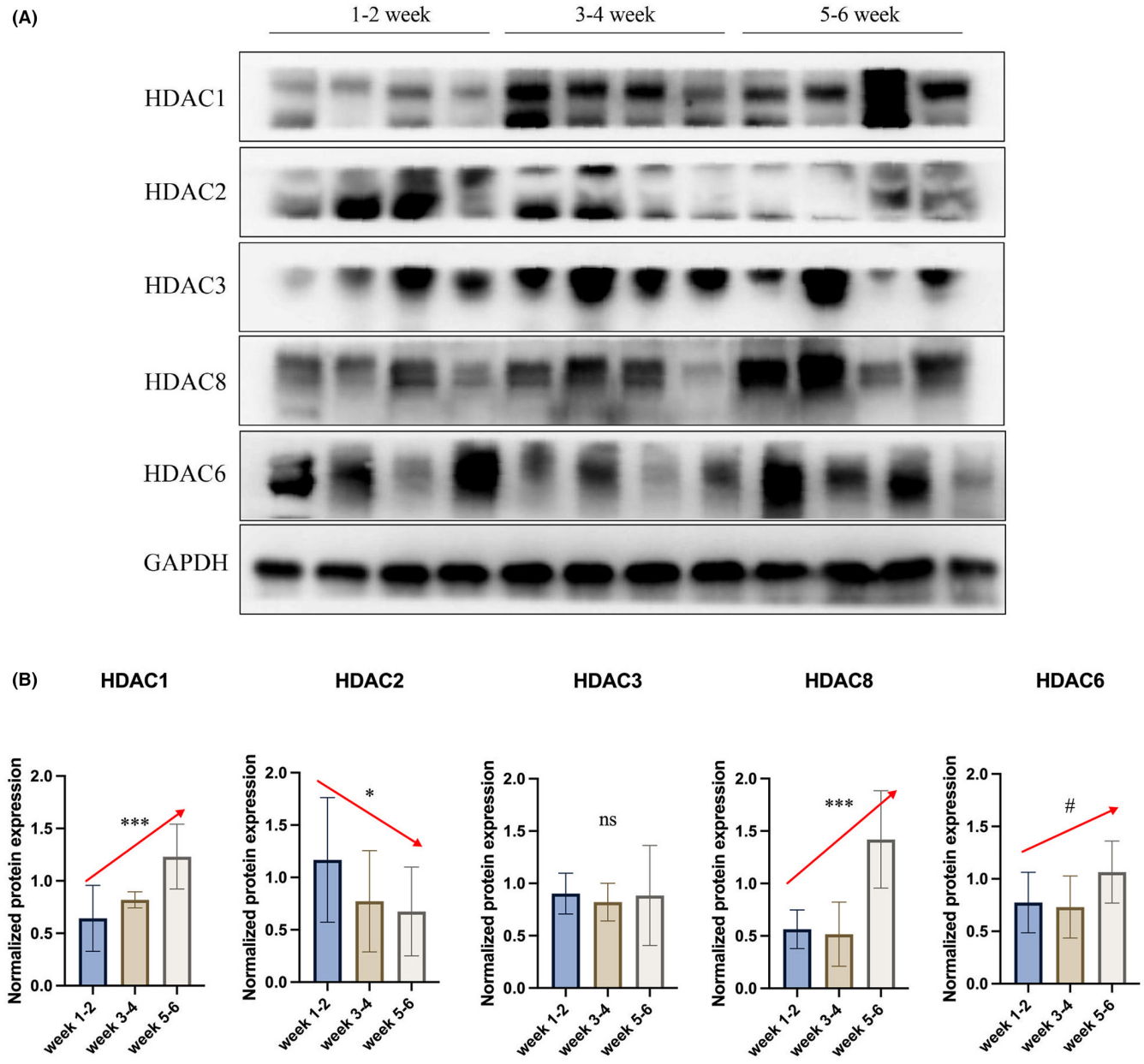

FIGURE 4 Western blot detection (A) and data analysis (B) of Class I HDACs (Hdac1-3 and Hdac8) and Hdac6 expression in early (1–2 weeks), middle (3–4 weeks), and late (5–6 weeks) stages of lesions harvested serially from endometriotic lesions of mice during the progression of endometriosis in Experiment 1. The data are represented by the means ± SDs. The arrow indicates a statistically significant linear trend based on linear regression analysis. Symbols of statistical significance levels: #: $0.05 < p < 0.1$; *: $p < 0.05$; ***: $p < 0.001$; NS: not statistically significant ($p > 0.05$). $N = 8$ in each group. Linear regression analysis was employed with the "age" of lesions, that is, early, middle, and late being coded as 1, 2, and 3.

Because the stromal component constituted the larger portion than glandular epithelial component in all lesions, and because both "young" and "old" lesions exhibited significantly lower Hdac3 staining than that of control endometrium, no difference in protein expression levels of Hdac3 should be expected between "younger" and "older" lesions.

Therefore, we concluded that among all Class I HDACs and Hdac6, both Hdac1 and Hdac8 are most likely to play a vital role in the progression of endometriotic lesions in mice. Hdac2 may also be involved.

3.2 | Hdac8 activation accelerates lesional progression and fibrogenesis

To see whether Hdac8 upregulation indeed promotes lesional development and fibrogenesis, we conducted the second mouse experiment and evaluated the effect of Hdac8 activation through its activator, TM-2-51.

No mouse died during the experiment, and no noticeable adverse effect occurred. TM-2-51 (20 mg/kg/day) appeared to be well tolerated in treated mice. Endometriosis was successfully

induced and histologically confirmed by H&E staining. While by the end of the experiment, the bodyweight of mice in both treated and untreated groups increased significantly as compared with that before the induction of endometriosis (both p-values ≤0.008), no significant difference in bodyweight was found between the two groups before the induction of endometriosis, before the treatment, and 4 weeks after the induction (all p-values ≥0.13; Figure 5A).

There was no difference in hotplate latency before the induction of endometriosis and 2 weeks after the induction ($p=0.72$ and $p=0.65$, respectively; Figure 5B). Four weeks after the induction, both groups of mice had significantly reduced latency as compared with their respective pre-induction levels (both p-values ≤0.016; Figure 5B). However, mice that received i.p. administration with TM-2-51 had significantly shorter latency as compared to that of the untreated group ($p=0.038$; Figure 5B). Consistently, the lesion weight in mice who received TM-2-51 treatment was nearly 3-fold heavier than that of control mice (153.0 ± 50.6 mg vs. 53.4 ± 25.8 mg, $p=0.0002$; Figure 5C).

To gain more insight into the possible mechanisms underlying the acceleration effect of TM-2-51, we further performed immunohistochemical analysis of E-cadherin, α-Sma, desmin, Sm-mhc, and

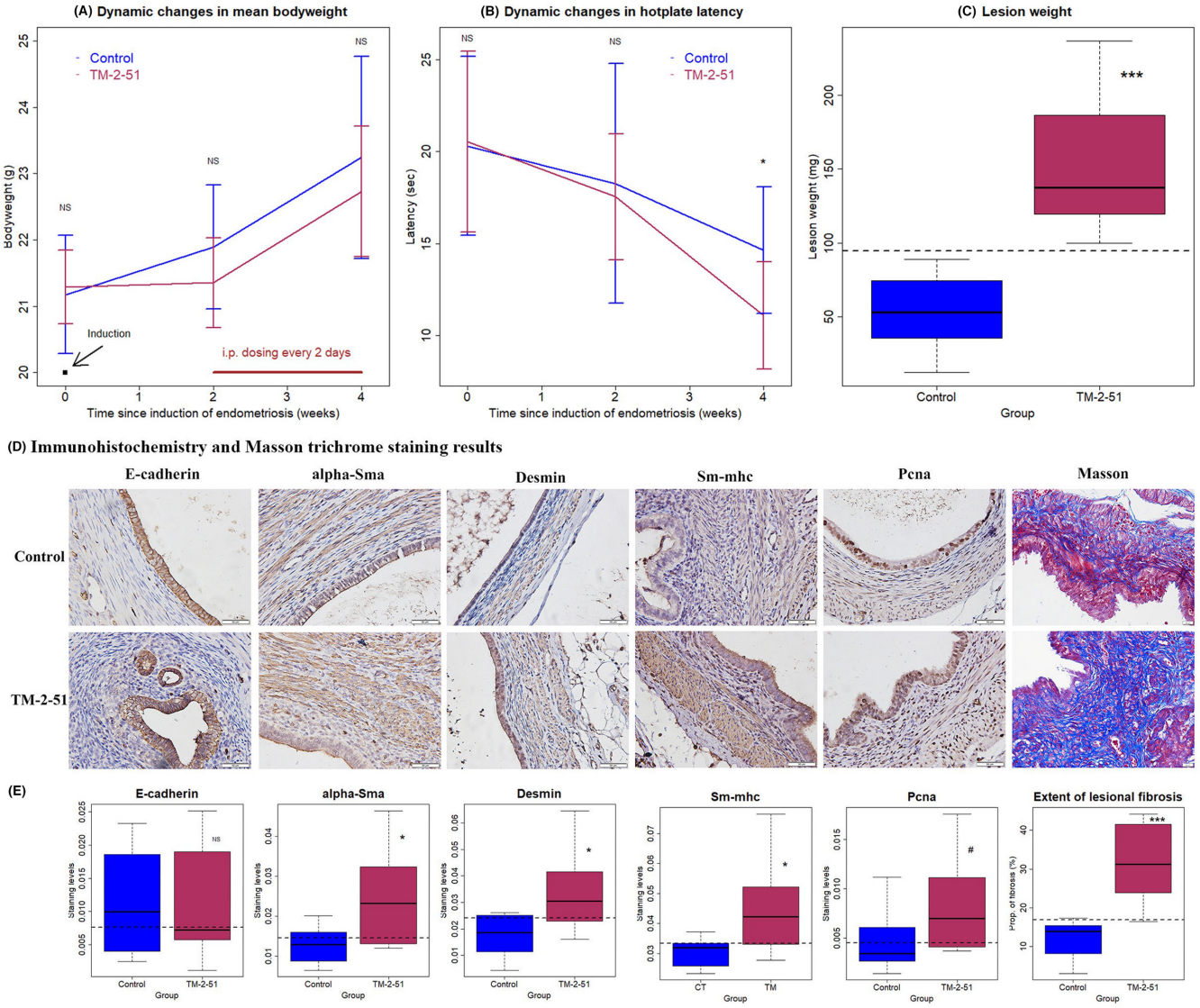

FIGURE 5 (A) Dynamic changes in the mean bodyweight between vehicle and TM-2-51-treated mice in Experiment 2. (B) Dynamic changes in the mean hotplate latency between two groups of mice. (C) Total lesion weight between two groups of mice. In all panels, the data are represented by the means ± SDs. N = 8 for each group. In panels (A) and (B), the Kruskal–Wallis test was used, while the Mann–Whitney test was used in panel (C). (D) Representative photomicrographs of immunostaining and Masson trichrome staining in Experiment 2. Different rows represent different tissue samples from endometriotic lesions taken from control mice and mice treated with TM-2-51. Different columns show different markers as indicated. All mice were induced with endometriosis. In Masson trichrome staining, the collagen fibers in lesions were stained in blue. In all figures, magnification: ×400. Scale bar = 50 μm. (E) Data summary of immunostaining and Masson trichrome staining. $N=8$ for each group. Symbols of statistical significance levels: #: $0.05<p<0.1$; *: $p<0.05$; ***: $p<0.001$; NS: not statistically significant ($p>0.05$). The Wilcoxon test was used in all panels.

Pcna for endometriotic lesions, as well as histological quantification of the extent of fibrosis by Masson trichrome staining (Figure 5D). With the only exception of E-cadherin (p = 0.96), we found that the mice in the TM-2-51-treated group showed a significantly elevated immunoexpression of α-Sma, desmin, and Sm-mhc as compared to the CTL group (all *p*-values ≤0.038; Figure 5E). The lesional staining level of Pcna was also elevated in the TM-2-51-treated group, but the difference was marginally significant ($p = 0.052$; Figure 5E). Similarly, the extent of lesional fibrosis in the TM-2-51 mice was significantly higher than that in the CT group ($p = 0.0003$; Figure 5E).

The extent of lesional fibrosis correlated positively with the immunostaining levels of α-Sma ($r = 0.56$, $p = 0.025$) and desmin ($r = 0.59$, $p = 0.017$), as well as the lesion weight ($r = 0.75$, $p = 0.0008$) but correlated negatively with the hotplate latency ($r = -0.59$, $p = 0.016$). Thus, we conclude that the activation of Hdac8 through TM-2-51 is likely to facilitate the FMT and SMM processes, thereby promoting lesional fibrogenesis.

3.3 | Selective inhibition of Hdac6/8 impedes lesional progression and fibrogenesis

Given the elevated expression of Hdac8 and Hdac6 and thus their potential roles in endometriosis as shown above, we next carried out a mouse experiment to investigate the effects of specific inhibition of Hdac8 and Hdac6 individually. We used Tubastatin A (TUB), an HDAC6 specific inhibitor, and PCI-34051 (PCI), an HDAC8-specific inhibitor, on the development of endometriosis in mice.

No mouse died during the experiment, and no adverse effect was detected. Both TUB and PCI appeared to be well tolerated in treated mice. There was no difference in bodyweight among all groups of mice before and 1 week after the induction of endometriosis ($p = 0.96$, and $p = 0.56$, respectively), but the difference among all groups was marginally significant at the end of the experiment ($p = 0.055$; Figure 6A), due possibly to the difference between the CT and HP groups ($p = 0.016$). The gradual decrease in bodyweight in the CT group in contrast to other intervention groups was possibly due to the endometriosis-associated pain-suppressive food intake.[83] Note that, in contrast to Experiment 1, all mice in this experiment received daily i.p. injection which certainly caused pain on top of induced endometriosis, which may have exerted extra stress and thus suppressed food intake.[84] Therefore, the difference in bodyweight between CT and HP groups may be another piece of evidence of the effectiveness of PCI-34051 in alleviating endometriosis-associated pain.

We also evaluated the pain behavior of all mice using the hotplate test. As expected, we found no difference in hotplate latency before the start of treatment and before the induction of endometriosis (both *p*-values = 0.97; Figure 6B). One and 2 weeks after the induction, there was a marginally significant difference in latency ($p = 0.081$, and $p = 0.058$, respectively; Figure 6B). Two weeks after the induction, all groups of mice appeared to have decreased latency as compared to their respective pre-induction levels, but the difference was marginally significant in all groups except the HP group (*p*-values = 0.063 for the 5 groups and $p = 1.0$ for the HP group; Figure 6B). Multiple linear regression analysis using the difference in latency between the pre- and post-induction as the dependent variable and the dosage of TUB and PCI, the bodyweight, and the pre-induction latency as independent variables indicated that the pre-induction latency is negatively associated with, while the TUB and PCI dosages are positively associated with the change in latency ($p = 0.0008$, $p = 0.020$, and $p = 0.0003$, respectively; $R^2 = 0.61$).

We found no visible endometriotic lesions in two mice from the LP group and one from the HP group. The lesion weight correlated positively with the hotplate latency ($r = -0.59$, $p = 0.002$). Compared with the CT mice, the average lesion weight in LT, HT, LP, and HP groups was reduced by 51.5%, 70.2%, 82.1%, and 85.7%, respectively (Figure 6C), suggesting potent and dose-dependent suppression of lesion growth by the treatment of inhibitors, especially that of HDAC8. Except for the LT and HT groups ($p = 0.096$, and $p = 0.059$, respectively), mice in both dosages of PCI groups had significantly lower lesion weight than the CT mice ($p = 0.031$ and $p = 0.036$, respectively; Figure 6C). Multiple linear regression analysis of lesion weight using the dosages of TUB and PCI, and the bodyweight as independent variables indicated that hotplate latency is positively associated with, while the TUB and PCI dosages are negatively associated with the lesion weight ($p = 0.024$, $p = 0.006$, and $p = 0.0004$, respectively; $R^2 = 0.47$).

To gain insight into the possible mechanisms underlying the suppressive effect of the above inhibitors, we also performed IHC analyses. We analyzed the expression of Pcna (a marker for proliferation), E-cadherin (a marker for epithelial cells), vimentin (a marker for mesenchymal cells), and α-Sma (a marker for myofibroblasts) in ectopic lesions. In addition, we evaluated the extent of lesional as well as endometrial fibrosis by Masson trichrome staining. Pcna stained positively in cellular nuclei in stromal and epithelial cells (Figure 7). E-cadherin staining was seen mostly in the cytoplasm and membranes in epithelial cells, and that of vimentin and α-Sma was in the cytoplasm in both stromal and epithelial cells (Figure 7).

Using regression analysis incorporating the dosage of TUB and of PCI as two covariables, we found that treatment with TUB and PCI both dose-dependently reduced the lesional staining of Pcna ($p = 0.025$ and $p = 0.0011$, $R^2 = 0.46$), vimentin ($p = 0.039$ and $p = 0.0013$, $R^2 = 0.46$), and α-Sma ($p = 0.031$ and $p = 0.0039$, $R^2 = 0.39$), as well as the extent of lesional fibrosis ($p = 0.046$ and $p = 0.0026$, $R^2 = 0.41$; Figure 7). However, treatment with PCI, but not TUB, was found to increase the lesional staining levels of E-cadherin ($p = 0.030$, $R^2 = 0.26$) and reduce the extent of endometrial fibrosis ($p = 0.015$, $R^2 = 0.30$; Figure 7). The extent of endometrial fibrosis seemed to be higher in CT mice as compared to other groups, irrespective the estrous cycle (Figure S3).

As expected, lesional staining of Pcna correlated positively with the lesion weight ($r = 0.51$, $p = 0.018$). The extent of lesional fibrosis correlated positively with the lesion weight ($r = 0.81$, $p = 1.0 \times 10^{-5}$) and lesional staining levels of vimentin ($r = 0.67$, $p = 0.0013$), but

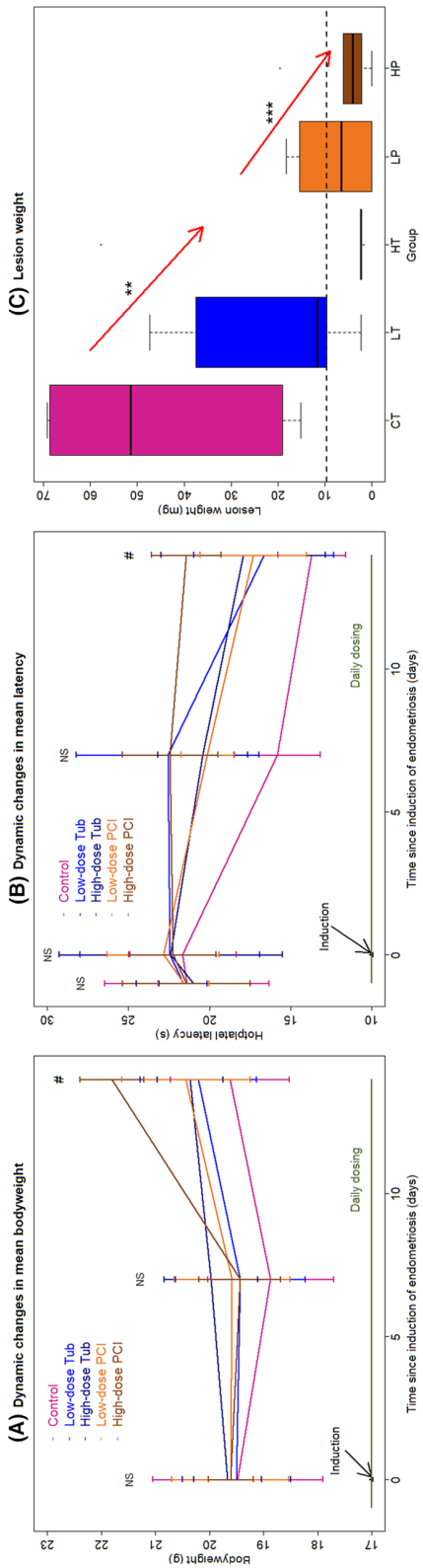

FIGURE 6 Dynamic changes in the mean bodyweight (A) and the mean hotplate plate latency (B) among five different groups of mice in Experiment 3. In both (A) and (B), the data are represented by the means ± SDs, and the time point at which endometriosis was induced is indicated by an arrow. The start time and the duration of the treatment of specific HDAC8 or HDAC6 inhibitor or just vehicle also is indicated. (C) Boxplot showing the total lesion weight among five different groups of mice. The dashed line is the median value of all groups. The red arrows represent a statistically significant dose-dependent trending by linear regression analysis using dosage as an independent variable. Symbols of statistical significance levels: #: $0.05 < p < 0.1$; *: $p < 0.05$; **: $p < 0.01$; ***: $p < 0.001$; NS: $p > 0.1$. $N = 5$ for each group. LT, low-dose Tubastatin A (20 mg/kg/day); HT, high-dose Tubastatin A (40 mg/kg/day); LP, low-dose PCI-34051 (10 mg/kg/day); HP, high-dose PCI-34051 (20 mg/kg/day).

negatively with the hotplate latency ($r = -0.51$, $p = 0.017$). It also correlated negatively with lesional staining levels of E-cadherin ($r = -0.34$, $p = 0.14$) but positively with α-Sma ($r = 0.37$, $p = 0.10$), but the correlation coefficient did not reach a statistically significant level.

Thus, treatment with TUB or PCI, especially PCI, attenuated cellular proliferation and impeded EMT and FMT of endometriotic lesions, resulting in decelerated lesional fibrogenesis. In addition, PCI treatment also attenuated fibrogenesis in endometrium resulting from endometriosis.

4 | DISCUSSION

Through a serial experiment involving mice with induced endometriosis, we found a significant and progressive increase in lesional staining of Hdac1, Hdac8, and Hdac6 as compared to normal endometrium and gradual decrease in Hdac2 staining and consistently reduced staining of Hdac3 during the course of lesional progression. Of note, the stromal Hdac8 staining correlated most prominently with all markers of lesional fibrosis (Figure S2C,I–K), suggesting that Hdac8 may play important roles in lesional fibrogenesis. Consistently, the Hdac1 and Hdac8 expression levels of proteins extracted from the lesional tissues were found to be lesional "age"-dependently elevated. In addition, Hdac8 activation significantly accelerated the progression and fibrogenesis of endometriotic lesions. In contrast, specific inhibition of Hdac8 or Hdac6, especially of Hdac8, significantly hindered lesional progression and fibrogenesis.

Our findings are consistent with the previous reports that lesional Hdac1 expression is significantly elevated as compared to that of control endometrium.[16,44] The finding of no change in Hdac2 staining in early lesions may be in agreement with the previous report,[16] but the finding of significantly reduced in "older" lesions is consistent with our own human data (Zheng et al., submitted for publication). These nuanced staining results are suggestive of Hdac2 downregulation when lesions are fibrotic and may be able to explain the conflicting results on HDAC2.[16,44] In addition, our findings are consistent with our human data indicating that lesional expression of HDAC1, HDAC8, and HDAC6 are significantly elevated as compared to that of normal endometrium (Zheng et al., submitted for publication).

Our results of reduced Hdac3 expression in endometriotic lesions are consistent with our observation in human endometriosis (Zheng et al., submitted for publication), and also with our recent finding that increased stiffness in culture substrate reduces the expression of HDAC3 (Mao et al., submitted for publication). This is in line with the report that increased substrate stiffness reduces the HDAC2 expression[85] since increased fibrotic content in lesions begets lesional rigidity. However, our results correct the claim that only HDAC1, but no other Class I HDACs, is aberrantly expressed in endometriotic lesions.[16]

Our results also are self-consistent, in that the results of our protein expression quantification experiment were in broad agreement

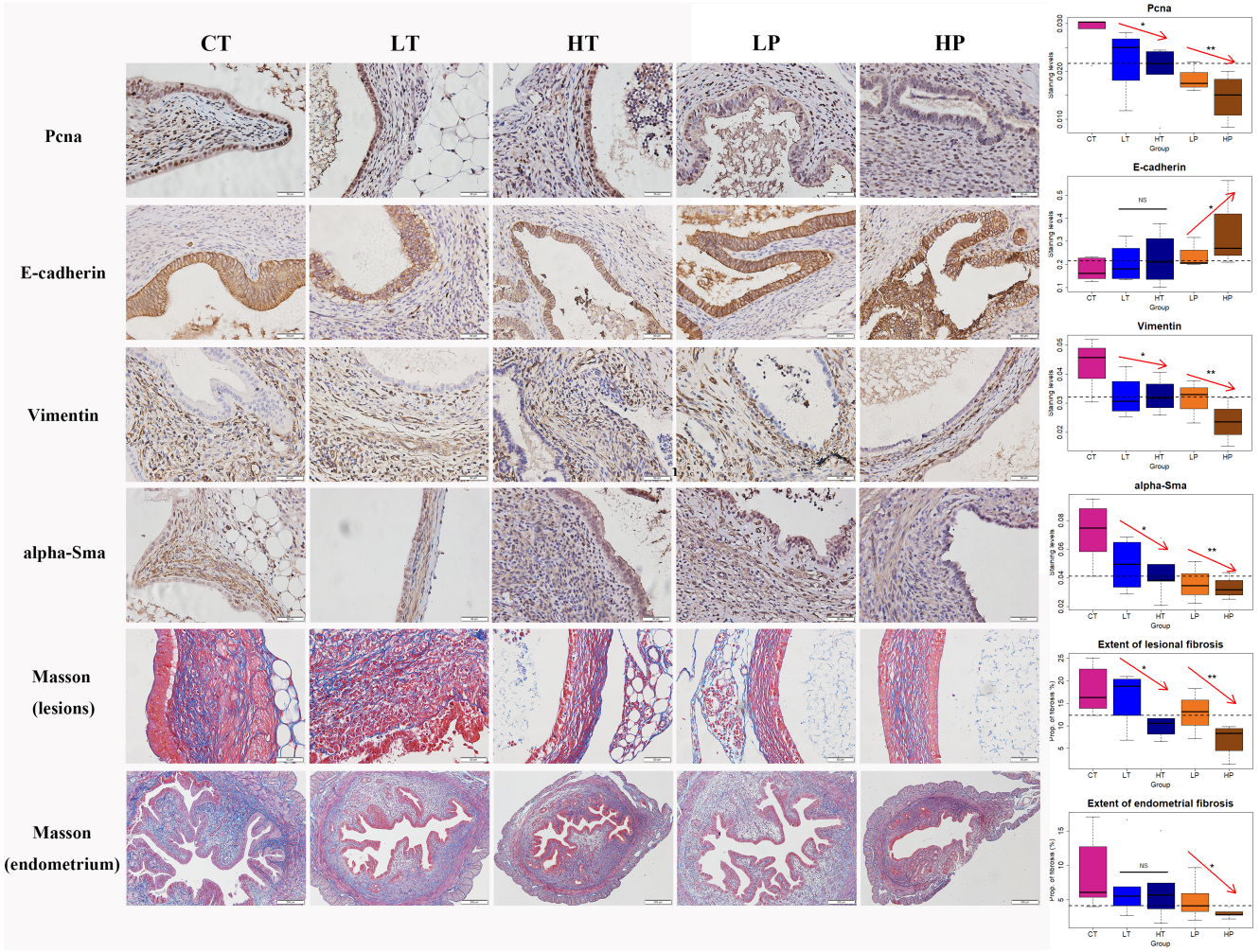

FIGURE 7 Representative photomicrographs of immunostaining and Masson trichrome staining analysis of endometriotic lesions from five different groups in Experiment 3. Different rows show different markers as indicated. Different columns represent different tissue samples from control mice and mice treated with a low or high dose of HDAC6 and HDAC8 inhibitor. In Masson trichrome staining, the collagen fibers in lesions were stained blue. In all figures except for endometrial fibrosis, magnification: ×400. Scale bar = 50 μm. In figures for endometrial fibrosis, magnification: ×100. Scale bar = 200 μm. Boxplot of Pcna, E-cadherin, vimentin, α-Sma, and extent of lesional and endometrial fibrosis among ectopic lesions from control mice and mice treated with a low- or high dose of HDAC6 and HDAC8 inhibitor, respectively. In all panels, the data are represented by the means ± SDs. The dashed line is the median value of all groups. The red arrows represent a statistically significant dose-dependent trending by linear regression analysis using dosage as an independent variable. The flat line indicates no significant trending. Symbols of statistical significance levels: *: $p < 0.05$; **: $p < 0.01$; NS: not statistically significant ($p > 0.05$). LT, low-dose Tubastatin A (20 mg/kg/day); HT, high-dose Tubastatin A (40 mg/kg/day); LP, low-dose PCI-34051 (10 mg/kg/day); HP, high-dose PCI-34051 (20 mg/kg/day).

with that of IHC analysis. For example, the "age"-dependent increase in Hdac8 protein levels as lesions progressed is consistent with the IHC finding of a linearly increasing trend (Figure S2C,D), even though in the IHC analysis the epithelial and the stromal components were scored separately while in the quantification of Hdac8 proteins, no such distinction regarding cell types was made. In addition, the apparent no change in Hdac3 staining in both epithelial and stromal components as lesions progressed agrees with the IHC finding of no difference in Hdac3 proteins for lesions of different "ages" (Figure 4B). The proteins were extracted from the lesion tissues, which consisted not only of endometriotic epithelial and stromal cells but also endothelial cells and immune cells.

Hdac8 has been reported to be involved in smooth muscle differentiation in normal human tissues and interacts with α-Sma and Sm-mhc,[86,87] and regulates SMC contraction.[88] It is thus not surprising that Hdac8 staining is progressively elevated in endometriotic lesions, which undergo SMM during lesional fibrogenesis.[60,61] Our research on the exact mechanism underlying Hdac8-mediated lesional fibrogenesis is ongoing, but its facilitatory role in lesional progression appears to be certain.

Remarkably, despite the fact that HDACIs have been consistently shown in preclinical studies by many groups to be a promising therapeutic for treating endometriosis,[13,26–39] our knowledge as the specific roles of each and individual HDAC is still incomplete

at best. Even for the most investigated Class I HDACs, while HDAC1 upregulation seems to be the consensus, the roles of other members of Class I HDACs are unclear and often conflicting.[16,44] As the drug development for non-hormonal therapeutics for endometriosis is fraught with abject failure,[5] and as the HDACIs have been shown to possess many desirable properties such as suppression of uterine contraction,[32,47] inflammation,[49] and neuropathic pain[89,90] and anti-fibrosis,[50–54] we hope that our finding of HDAC8 (and possibly HDAC6) overexpression and reaffirmation of HDAC1 overexpression in endometriotic lesions should hopefully rekindle the interest in targeting the epigenetic aberration in endometriosis.

The biggest strength of this study is the serial observation of cellular changes in endometriotic lesions in conjunction with the changes in immunostaining of Class I HDACs and Hdac6. This, coupled with the experiment demonstrating the lesion-promotional role of Hdac8 activation and the experiment showing the progression-arresting effect of Hdac8 or Hdac6 inhibition, provides credible experimental evidence for the role of Hdac8 in lesional progression and fibrogenesis. Indeed, our human data also found aberrant overexpression of HDAC8 in endometriotic lesions and an in vivo experiment demonstrated a promising therapeutic potential of HDAC8 suppression in a mouse model of deep endometriosis (Zheng et al., submitted for publication).

This study also has several limitations. First, the sample sizes at each tissue harvest time point used in the serial experiment are rather moderate, which may yield inadequate statistical power to detect genuine and important differences. This problem is partially remedied by the use of linear regression modeling incorporating all observations, but larger sample sizes should provide more precise estimates. Secondly, while the use of immunohistochemistry analysis provides a convenient way to ascertain the cell type, location, and expression levels of select markers, it cannot determine whether the protein is expressed or secreted by other neighboring cells. Thirdly, we did not include a control group in the quantification of protein levels for the serial experiment, nor did we extracted proteins from a specific cell type. Lastly, we did not specifically investigate the effect of Hdac6 activation on lesional development. Future studies are warranted to illuminate these issues.

In conclusion, through a serial mouse experiment and the evaluation of the effect of Hdac8 activation and of suppression, we have demonstrated that Hdac8 is aberrantly upregulated in endometriosis, likely facilitating lesional progression and fibrogenesis. This, along with the documented HDAC1 upregulation in endometriosis and the overwhelming evidence for the therapeutic potentials of HDACIs, calls for further and in-depth investigation of epigenetic aberrations of endometriosis in general and of HDACs in particular.

ACKNOWLEDGMENTS

This research was supported in part by grant 82071623 (SWG) from the National Natural Science Foundation of China and grant SHDC2020CR2062B from Shanghai Shenkang Center for Hospital Development. We would like to thank Dr. Jing Dong for her expert and selfless help in procuring tissue samples and experimentation.

CONFLICT OF INTEREST STATEMENT

S.W.G. is a member of the Scientific Advisory Board of Heranova BioSciences and has provided consultancy advice to the company, as well as to Sound Bioventures and BioGeneration, but these activities had no bearing on this work. All authors state that they have no competing interest.

ANIMAL WELFARE

All experiments involving animals as shown in this manuscript have been demonstrated to be ethically acceptable and where relevant conform to appropriate national guidelines for animal usage in research.

ORCID

Sun-Wei Guo https://orcid.org/0000-0002-8511-7624

REFERENCES

1. Vercellini P, Vigano P, Somigliana E, Fedele L. Endometriosis: pathogenesis and treatment. Nat Rev Endocrinol. 2014;10(5):261–75.
2. Bulun SE. Endometriosis. N Engl J Med. 2009;360(3):268–79.
3. Vercellini P, Buggio L, Frattaruolo MP, Borghi A, Dridi D, Somigliana E. Medical treatment of endometriosis-related pain. Best Pract Res Clin Obstet Gynaecol. 2018;51:68–91.
4. Giudice LC, Kao LC. Endometriosis. Lancet. 2004;364(9447):1789–99.
5. Guo SW, Groothuis PG. Is it time for a paradigm shift in drug research and development in endometriosis/adenomyosis? Hum Reprod Update. 2018;24(5):577–98.
6. Wu Y, Halverson G, Basir Z, Strawn E, Yan P, Guo SW. Aberrant methylation at HOXA10 may be responsible for its aberrant expression in the endometrium of patients with endometriosis. Am J Obstet Gynecol. 2005;193(2):371–80.
7. Guo SW. Epigenetics of endometriosis. Mol Hum Reprod. 2009;15(10):587–607.
8. Nasu K, Kawano Y, Kai K, Aoyagi Y, Abe W, Okamoto M, et al. Aberrant histone modification in endometriosis. Front Biosci. 2014;19:1202–14.
9. Borghese B, Zondervan KT, Abrao MS, Chapron C, Vaiman D. Recent insights on the genetics and epigenetics of endometriosis. Clin Genet. 2017;91(2):254–64.
10. Wu Y, Strawn E, Basir Z, Halverson G, Guo SW. Promoter hypermethylation of progesterone receptor isoform B (PR-B) in endometriosis. Epigenetics. 2006;1(2):106–11.
11. Xue Q, Lin Z, Cheng YH, Huang CC, Marsh E, Yin P, et al. Promoter methylation regulates estrogen receptor 2 in human endometrium and endometriosis. Biol Reprod. 2007;77(4):681–7.
12. Xue Q, Lin Z, Yin P, Milad MP, Cheng YH, Confino E, et al. Transcriptional activation of steroidogenic factor-1 by hypomethylation of the 5' CpG Island in endometriosis. J Clin Endocrinol Metab. 2007;92(8):3261–7.
13. Jichan N, Xishi L, Guo SW. Promoter hypermethylation of progesterone receptor isoform B (PR-B) in adenomyosis and its rectification by a histone deacetylase inhibitor and a demethylation agent. Reprod Sci. 2010;17(11):995–1005.
14. Izawa M, Harada T, Taniguchi F, Ohama Y, Takenaka Y, Terakawa N. An epigenetic disorder may cause aberrant expression of aromatase gene in endometriotic stromal cells. Fertil Steril. 2008;89(5 Suppl):1390–6.
15. Izawa M, Taniguchi F, Uegaki T, Takai E, Iwabe T, Terakawa N, et al. Demethylation of a nonpromoter cytosine-phosphate-guanine Island in the aromatase gene may cause the aberrant up-regulation in endometriotic tissues. Fertil Steril. 2011;95(1):33–9.

16. Samartzis EP, Noske A, Samartzis N, Fink D, Imesch P. The expression of histone deacetylase 1, but not other class I histone deacetylases, is significantly increased in endometriosis. Reprod Sci. 2013;20(12):1416–22.
17. Liu X, Nie J, Guo SW. Elevated immunoreactivity against class I histone deacetylases in adenomyosis. Gynecol Obstet Invest. 2012;74(1):50–5.
18. Wu Y, Strawn E, Basir Z, Halverson G, Guo SW. Aberrant expression of deoxyribonucleic acid methyltransferases DNMT1, DNMT3A, and DNMT3B in women with endometriosis. Fertil Steril. 2007;87(1):24–32.
19. Liu X, Guo SW. Aberrant immunoreactivity of deoxyribonucleic acid methyltransferases in adenomyosis. Gynecol Obstet Invest. 2012;74(2):100–8.
20. Ding D, Liu X, Guo SW. Overexpression of lysine-specific demethylase 1 in ovarian endometriomas and its inhibition reduces cellular proliferation, cell cycle progression, and invasiveness. Fertil Steril. 2014;101(3):740–9.
21. Sun Q, Ding D, Liu X, Guo SW. Tranylcypromine, a lysine-specific demethylase 1 (LSD1) inhibitor, suppresses lesion growth and improves generalized hyperalgesia in mouse with induced endometriosis. Reprod Biol Endocrinol. 2016;14:17.
22. Zhang Q, Dong P, Liu X, Sakuragi N, Guo SW. Enhancer of Zeste homolog 2 (EZH2) induces epithelial-mesenchymal transition in endometriosis. Sci Rep. 2017;7(1):6804.
23. Liu X, Zhang Q, Guo SW. Histological and Immunohistochemical characterization of the similarity and difference between ovarian Endometriomas and deep infiltrating endometriosis. Reprod Sci. 2018;25(3):329–40.
24. Colon-Caraballo M, Torres-Reveron A, Soto-Vargas JL, Young SL, Lessey B, Mendoza A, et al. Effects of histone methyltransferase inhibition in endometriosis. Biol Reprod. 2018;99(2):293–307.
25. Brunty S, Ray Wright K, Mitchell B, Santanam N. Peritoneal modulators of EZH2-miR-155 cross-talk in endometriosis. Int J Mol Sci. 2021;22(7):3492.
26. Wu Y, Guo SW. Histone deacetylase inhibitors trichostatin a and valproic acid induce cell cycle arrest and p21 expression in immortalized human endometrial stromal cells. Eur J Obstet Gynecol Reprod Biol. 2008;137(2):198–203.
27. Wu Y, Guo SW. Suppression of IL-1beta-induced COX-2 expression by trichostatin a (TSA) in human endometrial stromal cells. Eur J Obstet Gynecol Reprod Biol. 2007;135(1):88–93.
28. Wu Y, Starzinski-Powitz A, Guo SW. Trichostatin a, a histone deacetylase inhibitor, attenuates invasiveness and reactivates E-cadherin expression in immortalized endometriotic cells. Reprod Sci. 2007;14(4):374–82.
29. Liu M, Liu X, Zhang Y, Guo SW. Valproic acid and progestin inhibit lesion growth and reduce hyperalgesia in experimentally induced endometriosis in rats. Reprod Sci. 2012;19(4):360–73.
30. Liu X, Guo SW. Valproic acid alleviates generalized hyperalgesia in mice with induced adenomyosis. J Obstet Gynaecol Res. 2011;37(7):696–708.
31. Lu Y, Nie J, Liu X, Zheng Y, Guo SW. Trichostatin a, a histone deacetylase inhibitor, reduces lesion growth and hyperalgesia in experimentally induced endometriosis in mice. Hum Reprod. 2010;25(4):1014–25.
32. Mao X, Wang Y, Carter AV, Zhen X, Guo SW. The retardation of myometrial infiltration, reduction of uterine contractility, and alleviation of generalized hyperalgesia in mice with induced adenomyosis by levo-tetrahydropalmatine (l-THP) and andrographolide. Reprod Sci. 2011;18(10):1025–37.
33. Imesch P, Samartzis EP, Dedes KJ, Fink D, Fedier A. Histone deacetylase inhibitors down-regulate G-protein-coupled estrogen receptor and the GPER-antagonist G-15 inhibits proliferation in endometriotic cells. Fertil Steril. 2013;100(3):770–6.
34. Imesch P, Fink D, Fedier A. Romidepsin reduces histone deacetylase activity, induces acetylation of histones, inhibits proliferation, and activates apoptosis in immortalized epithelial endometriotic cells. Fertil Steril. 2010;94(7):2838–42.
35. Imesch P, Samartzis EP, Schneider M, Fink D, Fedier A. Inhibition of transcription, expression, and secretion of the vascular epithelial growth factor in human epithelial endometriotic cells by romidepsin. Fertil Steril. 2011;95(5):1579–83.
36. Seo SK, Lee JH, Chon SJ, Yun BH, Cho S, Choi YS, et al. Trichostatin a induces NAG-1 expression and apoptosis in human Endometriotic stromal cells. Reprod Sci. 2018;25(9):1349–56.
37. Kai K, Nasu K, Kawano Y, Aoyagi Y, Tsukamoto Y, Hijiya N, et al. Death receptor 6 is epigenetically silenced by histone deacetylation in endometriosis and promotes the pathogenesis of endometriosis. Am J Reprod Immunol. 2013;70(6):485–96.
38. Kawano Y, Nasu K, Hijiya N, Tsukamoto Y, Amada K, Abe W, et al. CCAAT/enhancer-binding protein alpha is epigenetically silenced by histone deacetylation in endometriosis and promotes the pathogenesis of endometriosis. J Clin Endocrinol Metab. 2013;98(9):E1474–82.
39. Kawano Y, Nasu K, Li H, Tsuno A, Abe W, Takai N, et al. Application of the histone deacetylase inhibitors for the treatment of endometriosis: histone modifications as pathogenesis and novel therapeutic target. Hum Reprod. 2011;26(9):2486–98.
40. Liu X, Guo SW. A pilot study on the off-label use of valproic acid to treat adenomyosis. Fertil Steril. 2008;89(1):246–50.
41. Xishi L, Lei Y, Guo SW. Valproic acid as a therapy for adenomyosis: a comparative case series. Reprod Sci. 2010;17(10):904–12.
42. Audia JE, Campbell RM. Histone modifications and cancer. Cold Spring Harb Perspect Biol. 2016;8(4):a019521.
43. Tang J, Yan H, Zhuang S. Histone deacetylases as targets for treatment of multiple diseases. Clin Sci. 2013;124(11):651–62.
44. Colon-Diaz M, Baez-Vega P, Garcia M, Ruiz A, Monteiro JB, Fourquet J, et al. HDAC1 and HDAC2 are differentially expressed in endometriosis. Reprod Sci. 2012;19(5):483–92.
45. Mai H, Liao Y, Luo S, Wei K, Yang F, Shi H. Histone deacetylase HDAC2 silencing prevents endometriosis by activating the HNF4A/ARID1A axis. J Cell Mol Med. 2021;25(21):9972–82.
46. Kim TH, Yoo JY, Choi KC, Shin JH, Leach RE, Fazleabas AT, et al. Loss of HDAC3 results in nonreceptive endometrium and female infertility. Sci Transl Med. 2019;11(474):eaaf7533.
47. Moynihan AT, Hehir MP, Sharkey AM, Robson SC, Europe-Finner GN, Morrison JJ. Histone deacetylase inhibitors and a functional potent inhibitory effect on human uterine contractility. Am J Obstet Gynecol. 2008;199:167.
48. Karolczak-Bayatti M, Loughney AD, Robson SC, Europe-Finner GN. Epigenetic modulation of the protein kinase a RIIalpha (PRKAR2A) gene by histone deacetylases 1 and 2 in human smooth muscle cells. J Cell Mol Med. 2011;15(1):94–108.
49. Han SB, Lee JK. Anti-inflammatory effect of Trichostatin-a on murine bone marrow-derived macrophages. Arch Pharm Res. 2009;32(4):613–24.
50. Khan S, Ahirwar K, Jena G. Anti-fibrotic effects of valproic acid: role of HDAC inhibition and associated mechanisms. Epigenomics. 2016;8(8):1087–1101.
51. Korfei M, Skwarna S, Henneke I, MacKenzie B, Klymenko O, Saito S, et al. Aberrant expression and activity of histone deacetylases in sporadic idiopathic pulmonary fibrosis. Thorax. 2015;70(11):1022–32.
52. Seet LF, Chu SW, Toh LZ, Teng X, Yam GH, Wong TT. Valproic acid modulates collagen architecture in the postoperative conjunctival scar. J Mol Med. 2022;100(6):947–61.
53. Costalonga EC, de Freitas LJ, Aragone D, Silva FMO, Noronha IL. Anti-fibrotic effects of valproic acid in experimental peritoneal fibrosis. PloS One. 2017;12(9):e0184302.

54. Kawaoka K, Doi S, Nakashima A, Yamada K, Ueno T, Doi T, et al. Valproic acid attenuates renal fibrosis through the induction of autophagy. Clin Exp Nephrol. 2017;21:771–80.
55. Guo SW, Mao X, Ma Q, Liu X. Dysmenorrhea and its severity are associated with increased uterine contractility and overexpression of oxytocin receptor (OTR) in women with symptomatic adenomyosis. Fertil Steril. 2013;99(1):231–40.
56. Vigano P, Candiani M, Monno A, Giacomini E, Vercellini P, Somigliana E. Time to redefine endometriosis including its pro-fibrotic nature. Hum Reprod. 2018;33(3):347–52.
57. Guo SW. Fibrogenesis resulting from cyclic bleeding: the holy grail of the natural history of ectopic endometrium. Hum Reprod. 2018;33(3):353–6.
58. Gurvich N, Tsygankova OM, Meinkoth JL, Klein PS. Histone deacetylase is a target of valproic acid-mediated cellular differentiation. Cancer Res. 2004;64(3):1079–86.
59. Sixto-Lopez Y, Bello M, Correa-Basurto J. Exploring the inhibitory activity of valproic acid against the HDAC family using an MMGBSA approach. J Comput Aided Mol Des. 2020;34(8):857–78.
60. Zhang Q, Duan J, Liu X, Guo SW. Platelets drive smooth muscle metaplasia and fibrogenesis in endometriosis through epithelial-mesenchymal transition and fibroblast-to-myofibroblast transdifferentiation. Mol Cell Endocrinol. 2016;428:1–16.
61. Zhang Q, Duan J, Olson M, Fazleabas A, Guo SW. Cellular changes consistent with epithelial-mesenchymal transition and fibroblast-to-Myofibroblast Transdifferentiation in the progression of experimental endometriosis in baboons. Reprod Sci. 2016;23(10):1409–21.
62. Ding D, Wang X, Chen Y, Benagiano G, Liu X, Guo S-W. Evidence in support for the progressive nature of ovarian endometriomas. J Clin Endocrinol Metab. 2020;105(7):dgaa189.
63. Guo SW. Various types of adenomyosis and endometriosis: In search of optimal management. Fertil Steril. 2023;119(5):711–26.
64. Wu MH, Lu CW, Chuang PC, Tsai SJ. Prostaglandin E2: the master of endometriosis? Exp Biol Med (Maywood). 2010;235(6):668–77.
65. Huang Q, Liu X, Guo S-W. Changing prostaglandin E2 (PGE2) signaling during lesional progression and exacerbation of endometriosis by inhibition of PGE2 receptor EP2 and EP4. Reprod Med Biol. 2021;21(1):e12426.
66. Huang Q, Liu X, Guo SW. Higher fibrotic content of endometriotic lesions is associated with diminished prostaglandin E2 signaling. Reprod Med Biol. 2022;21(1):e12423.
67. National Research Council (US) Committee for the Update of the Guide for the Care and Use of Laboratory Animals. Guide for the care and use of laboratory animals. Washington, DC: National Academies Press; 2011.
68. Long Q, Liu X, Guo SW. Surgery accelerates the development of endometriosis in mice. Am J Obstet Gynecol. 2016;215(3):320.
69. Somigliana E, Vigano P, Rossi G, Carinelli S, Vignali M, Panina-Bordignon P. Endometrial ability to implant in ectopic sites can be prevented by interleukin-12 in a murine model of endometriosis. Hum Reprod. 1999;14(12):2944–50.
70. Singh RK, Cho K, Padi SK, Yu J, Haldar M, Mandal T, et al. Mechanism of N-Acylthiourea-mediated activation of human histone deacetylase 8 (HDAC8) at molecular and cellular levels. J Biol Chem. 2015;290(10):6607–19.
71. Chakrabarti A, Melesina J, Kolbinger FR, Oehme I, Senger J, Witt O, et al. Targeting histone deacetylase 8 as a therapeutic approach to cancer and neurodegenerative diseases. Future Med Chem. 2016;8(13):1609–34.
72. Shen S, Svoboda M, Zhang G, Cavasin MA, Motlova L, McKinsey TA, et al. Structural and in vivo characterization of Tubastatin a, a widely used histone deacetylase 6 inhibitor. ACS Med Chem Lett. 2020;11(5):706–12.
73. Géraldy M, Morgen M, Sehr P, Steimbach RR, Moi D, Ridinger J, et al. Selective inhibition of histone deacetylase 10: hydrogen bonding to the gatekeeper residue is implicated. J Med Chem. 2019;62(9):4426–43.
74. Li ML, Su XM, Ren Y, Zhao X, Kong LF, Kang J. HDAC8 inhibitor attenuates airway responses to antigen stimulus through synchronously suppressing galectin-3 expression and reducing macrophage-2 polarization. Respir Res. 2020;21(1):62.
75. Ren Y, Su X, Kong L, Li M, Zhao X, Yu N, et al. Therapeutic effects of histone deacetylase inhibitors in a murine asthma model. Inflamm Res. 2016;65(12):995–1008.
76. Mormino A, Cocozza G, Fontemaggi G, Valente S, Esposito V, Santoro A, et al. Histone-deacetylase 8 drives the immune response and the growth of glioma. Glia. 2021;69(11):2682–98.
77. Hendrix S, Sanchez S, Ventriglia E, Lemmens S. HDAC8 inhibition reduces Lesional Iba-1+ cell infiltration after spinal cord injury without effects on functional recovery. Int J Mol Sci. 2020;21(12):4539.
78. Zhou W, Yang J, Saren G, Zhao H, Cao K, Fu S, et al. HDAC6-specific inhibitor suppresses Th17 cell function via the HIF-1α pathway in acute lung allograft rejection in mice. Theranostics. 2020;10(15):6790–6805.
79. Zhang L, Liu C, Wu J, Tao JJ, Sui XL, Yao ZG, et al. Tubastatin a/ACY-1215 improves cognition in Alzheimer's disease transgenic mice. J Alzheimers Dis. 2014;41(4):1193–1205.
80. Zheng Y, Chen Y, Lu X, Weng Q, Dai G, Yu Y, et al. Inhibition of histone deacetylase 6 by Tubastatin a attenuates the Progress of osteoarthritis via improving mitochondrial function. Am J Pathol. 2020;190(12):2376–86.
81. R Core Team. R: a language and environment for statistical computing. Vienna, Austria: R Foundation for Statistical Computing; 2016.
82. Zhang Q, Liu X, Guo SW. Progressive development of endometriosis and its hindrance by anti-platelet treatment in mice with induced endometriosis. Reprod Biomed Online. 2017;34(2):124–36.
83. Huang Q, Liu X, Guo SW. Changing prostaglandin E2 (PGE(2)) signaling during lesional progression and exacerbation of endometriosis by inhibition of PGE(2) receptor EP2 and EP4. Reprod Med Biol. 2022;21(1):e12426.
84. Guo SW, Zhang Q, Liu X. Social psychogenic stress promotes the development of endometriosis in mouse. Reprod Biomed Online. 2017;34(3):225–39.
85. Li Y, Tang CB, Kilian KA. Matrix mechanics influence fibroblast-Myofibroblast transition by directing the localization of histone deacetylase 4. Cell Mol Bioeng. 2017;10(5):405–15.
86. Waltregny D, Glenisson W, Tran SL, North BJ, Verdin E, Colige A, et al. Histone deacetylase HDAC8 associates with smooth muscle alpha-Actin and is essential for smooth muscle cell contractility. FASEB J. 2005;19(8):966–8.
87. Waltregny D, De Leval L, Glenisson W, Ly Tran S, North BJ, Bellahcene A, et al. Expression of histone deacetylase 8, a class I histone deacetylase, is restricted to cells showing smooth muscle differentiation in normal human tissues. Am J Pathol. 2004;165(2):553–64.
88. Li J, Chen S, Cleary RA, Wang R, Gannon OJ, Seto E, et al. Histone deacetylase 8 regulates cortactin deacetylation and contraction in smooth muscle tissues. Am J Physiol-Cell Physiol. 2014;307(3):C288–95.
89. Matsushita Y, Araki K, Omotuyi O, Mukae T, Ueda H. HDAC inhibitors restore C-fibre sensitivity in experimental neuropathic pain model. Br J Pharmacol. 2013;170(5):991–8.

90. Pirapakaran K, Aggarwal A. The use of low-dose sodium valproate in the management of neuropathic pain: illustrative case series. Intern Med J. 2016;46(7):849–52.

SUPPORTING INFORMATION

Additional supporting information can be found online in the Supporting Information section at the end of this article.

How to cite this article: Zheng H, Liu X, Guo S-W. Corroborating evidence for aberrant expression of histone deacetylase 8 in endometriosis. Reprod Med Biol. 2023;22:e12527. https://doi.org/10.1002/rmb2.12527